J. Fluid Mech. (1985), *vol.* 151, *pp.* 1–20
Printed in Great Britain

On the ability of drops or bubbles to stick to non-horizontal surfaces of solids. Part 2. Small drops or bubbles having contact angles of arbitrary size

By E. B. DUSSAN V.
Department of Chemical Engineering, University of Pennsylvania, Philadelphia, PA 19104

(Received 27 February 1984 and in revised form 17 August 1984)

The ability of small drops or bubbles to stick to non-horizontal solid surfaces is analysed. The principal results consist of identifying the critical value of the volume of a drop (or bubble) beyond which it will dislodge and move down (or up) the surface of the solid, and determining the speed at which it will move. In addition, the area of the solid wetted by the drop (or dried by the bubble) is calculated when its volume is at its critical value. All of the results are expressed in terms of experimentally measurable material properties. The most limiting restriction on the validity of the results is the assumption that the value of the contact angle hysteresis is small.

1. Introduction

This represents an extension of the work presented in Dussan V. & Chow (1983), and thus it is entitled Part 2. Dussan V. & Chow limited their investigation to drops or bubbles† having shapes consistent with the small-slope approximation. Hence their results can only be used with material systems possessing small contact angles. This greatly limits the usefulness of their results. The objective of the present study is to extend their work to a case of practical importance, that of small drops with contact angles of arbitrary size. A significant number of the applications cited in §1 of Dussan V. & Chow fall into this category.

Specifically, Dussan V. & Chow were concerned with determining the size and shape of drops in their critical configuration. This they defined to be the largest drop that could stick to a solid surface inclined at a given angle. Also, they were concerned with predicting the speed at which drops roll down surfaces when either the angle of inclination of the solid or the volume of the drops slightly exceed their critical values. The key to their analysis was realizing that the contact line *must* contain straight-line segments (see figure 1). This is consistent with the experimental observations of Bikerman (1950) and Furmidge (1962). It is of interest to note that the boundary-value problems generated by the above contain boundary conditions of the mixed kind. That is to say, along the straight-line segments of the contact line, the local values of the contact angle are not known *a priori*; while, along the remainder of the contact line, the variation in value of the contact angle is given, however, the location of the contact line is part of the solution. The problem is further complicated by the fact that the locations of the ends of the straight-line segments are also part of the solution.

† For convenience, the material bodies of interest will henceforth be referred to as drops.

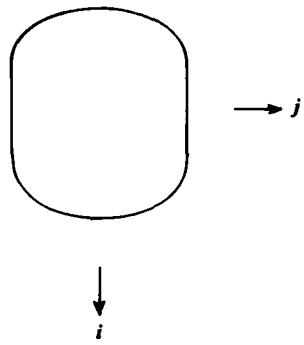

FIGURE 1. The general shape of the contact line is illustrated. The unit vector $\boldsymbol{i}$ points in the direction down the plate. Along both sides of the drop the contact line has straight-line segments.

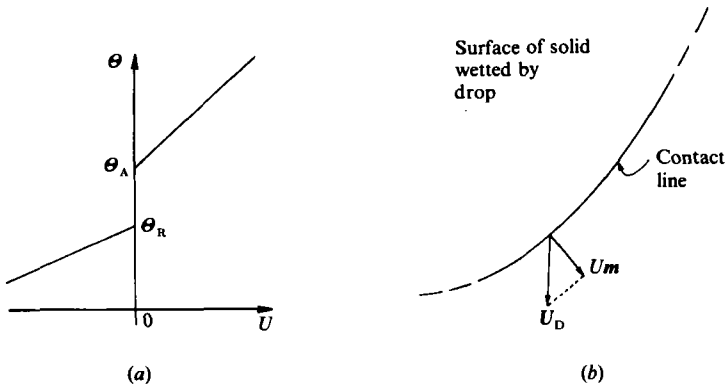

FIGURE 2. The value of the contact angle, which depends upon the speed U of the contact line, is assumed to have the form given in (*a*). The values of the slopes of the curve for $U > 0$ and $U < 0$ are $1/\kappa_A$ and $1/\kappa_R$ respectively. The speed of the contact line is $\boldsymbol{U}_D \cdot \boldsymbol{m}$, where $\boldsymbol{U}_D$ denotes the velocity of the drop, and $\boldsymbol{m}$ is a unit vector parallel to the solid surface, perpendicular to the local tangent vector to the contact line, and pointing away from the drop; see (*b*).

The central aspect of their model consisted of accounting for the mechanism by which the solid surface affects the drops. This was assumed to occur through the contact angle Θ. The specific model that they used and which will be used in this study is illustrated in figure 2. It contains *contact angle hysteresis*, a characteristic found in many material systems. This refers to the fact that the contact line will not move when the contact angle lies within the interval $[\Theta_R, \Theta_A]$. The two limiting static angles Θ_A and Θ_R are often referred to as the *advancing* and *receding contact angles* respectively. The model contains the simplifying feature in that the values of $d\Theta/dU$ for U over the range $(-\infty, 0)$ and $(0, +\infty)$, i.e. for both negative and positive contact line speeds, are assumed to be constant, although not necessarily equal. Their values will be denoted by $1/\kappa_R$ and $1/\kappa_A$, respectively. The values of all four parameters Θ_A, Θ_R, κ_A and κ_R must be experimentally determined.

The most direct way of differentiating the present study from that of Dussan V. & Chow is by identifying the range of validity of the relevant dimensionless groups. Both investigate the regular limits as both the Reynolds and capillary numbers†

† The definitions of the various dimensionless groups appear in §2.1.

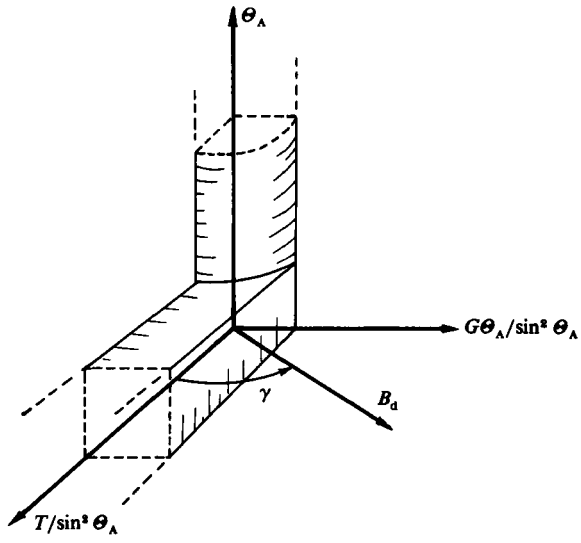

FIGURE 3. The regions of validity in parameter space of the two analyses are roughly indicated. A point in this space, using cylindrical coordinates, is given by (B_d, γ, Θ_A). The semi-infinite rectangular solid denotes the region of validity for the analysis of Dussan V. & Chow. The semi-infinite quarter of a cylinder represents the region of validity for the present study. They both overlap near the origin.

approach zero. Both are valid for arbitrary values of κ_A/κ_R, and assume that only a small amount of hysteresis is present. This latter assumption gives rise to an expansion in Dussan V. & Chow in terms of $(\Theta_A - \Theta_R)/\Theta_A$, which they found to have a singular limit as its value approaches zero. A significant portion of their presentation was devoted to determining the nature of this limit. In the present study $\cos\Theta_R - \cos\Theta_A$ appears as the natural small parameter. However, this change in parameter doesn't give rise to any significant change in the nature of the singularity, at least to lowest order. The chief differences between the two studies occur in the handling of the remaining three parameters: Θ_A, the Bond number B_d, and the angle of inclination γ of the surface of the solid with the horizontal. Dussan V. & Chow solve the lubrication equations which they found governs the lowest-order mode in an expansion in Θ_A as it approaches zero. This, of course, is not done in the present study. They also introduce the variables T and G, defined as $B_d \sin^2\Theta_A \cos\gamma$ and $(B_d \sin^2\Theta_A \sin\gamma)/\Theta_A$ respectively. Their results are valid for arbitrary values of T and for small values of G. The present study is restricted to small values of B_d. An illustration of the regions of validity of the two studies is given in figure 3.

The organization of the present study follows that of Dussan V. & Chow. In §2 the relevant dimensionless groups are defined, and expansions are performed. The case of a drop rolling down a surface with $\Theta_A \equiv \Theta_R$ is solved in §3. The size and shape of drops in their critical configuration is determined in §4. The results of these latter two sections are combined in §5 to describe a drop rolling down a surface in which $\Theta_A \not\equiv \Theta_R$, along with a general discussion.

2. Formulation

2.1. *Scaling and identification of boundary-value problem*

The scales for (x, y, z) are given by a_s. This denotes the radius of a spherical cap having the same volume as the drop and forming an angle of Θ_A with the surface of the solid. Its explicit definition is given by (2.13). The velocity $\boldsymbol{u}$ is scaled with κ_A. Pressure p is scaled with σ/a_s, where σ is the surface tension.

The Navier–Stokes and continuity equations in dimensionless form are

$$C_a R_e \boldsymbol{u}\cdot\nabla\boldsymbol{u} = -\nabla P + C_a \nabla^2\boldsymbol{u} - \boldsymbol{k} B_d \cos\gamma + \boldsymbol{i} B_d \sin\gamma \quad \text{and} \quad \nabla\cdot\boldsymbol{u} = 0$$

where the Reynolds number $R_e = \rho\kappa_A a_s/\mu$, the capillary number $C_a = \kappa_A \mu/\sigma$, and the Bond number, $B_d = \rho g a_s^2/\sigma$. Although the same symbol is used here for the Bond number as in Dussan V. & Chow, in fact they are not the same. Each is based upon a different lengthscale. Their relationship is given by $a = a_s \sin\Theta_A$, where a is the lengthscale appearing in Dussan V. & Chow.

The kinematic and dynamic boundary conditions at the free-surface are

$$\boldsymbol{u}\cdot\nabla_{II} R - \boldsymbol{u}\cdot\hat{\boldsymbol{r}} = 0 \quad \text{and} \quad -P + C_a \boldsymbol{n}\cdot[\nabla\boldsymbol{u} + \nabla\boldsymbol{u}^T]\cdot\boldsymbol{n} = \frac{1}{R_M},$$

where $r = R(\theta, \phi)$ denotes the location of the free-surface parametrized in terms of the spherical coordinates (r, θ, ϕ);

$$\nabla_{II}(\ ) \equiv \hat{\boldsymbol{\theta}}\frac{1}{r}\frac{\partial(\ )}{\partial\theta} + \hat{\boldsymbol{\phi}}\frac{1}{r\sin\theta}\frac{\partial(\ )}{\partial\phi},$$

with $\hat{\boldsymbol{r}}$, $\hat{\boldsymbol{\theta}}$ and $\hat{\boldsymbol{\phi}}$ denoting unit vectors along the three coordinate curves; and R_M denotes the mean radius of curvature of the free surface, given by

$$\begin{aligned}\frac{1}{R_M} = \Bigg[\Bigg\{\left(\frac{\partial R}{\partial\phi}\right)^2 + R^2\sin^2\theta\Bigg\}\Bigg\{\left(\frac{\partial^2 R}{\partial\theta^2} - R\right)R^2\sin\theta - 2R\left(\frac{\partial R}{\partial\theta}\right)^2\sin\theta\Bigg\} \\ + \Bigg\{\left(\frac{\partial R}{\partial\theta}\right)^2 + R^2\Bigg\}\Bigg\{\left(\frac{\partial^2 R}{\partial\phi^2} - R\sin^2\theta\right)R^2\sin\theta - 2R\left(\frac{\partial R}{\partial\phi}\right)^2\sin\theta + R^2\frac{\partial R}{\partial\theta}\sin^2\theta\cos\theta\Bigg\} \\ - 2\frac{\partial R}{\partial\phi}\frac{\partial R}{\partial\theta}\Bigg\{R^2\frac{\partial^2 R}{\partial\phi\,\partial\theta}\sin\theta - 2R\frac{\partial R}{\partial\theta}\frac{\partial R}{\partial\phi}\sin\theta - R^2\frac{\partial R}{\partial\phi}\cos\theta\Bigg\}\Bigg] \\ \times\Bigg[R^2\left(\frac{\partial R}{\partial\phi}\right)^2 + R^2\left(\frac{\partial R}{\partial\theta}\right)^2\sin^2\theta + R^4\sin^2\theta\Bigg]^{-\frac{3}{2}}. \end{aligned} \tag{2.1}$$

The coordinate system is oriented so that $\hat{\boldsymbol{r}}(\frac{1}{2}\pi, 0)$ and $\hat{\boldsymbol{r}}(\frac{1}{2}\pi, \frac{1}{2}\pi)$ lie tangent to the solid surface and equal $\boldsymbol{i}$ and $\boldsymbol{j}$, respectively, the vector $\boldsymbol{i}$ pointing in the direction of maximum descent. The solid surface is located at $z = \cos\Theta_A$, where the unit vector $\boldsymbol{k}$ is perpendicular to the surface pointing from the solid to the drop (see figure 4).

The kinematic and no-slip boundary conditions at the surface of the solid are given by

$$\boldsymbol{u} = \boldsymbol{U}_P,$$

where $\boldsymbol{U}_P$ denotes the velocity of the plate as viewed from a frame of reference at rest with respect to the centre of mass of the drop. Since we shall only be interested in the limit as both the Reynolds and capillary numbers approach zero, the analysis will be unaffected by the singularity arising from the no-slip boundary condition at the moving contact line.

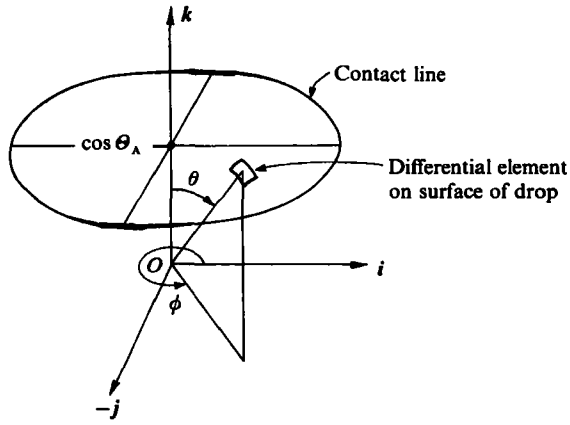

FIGURE 4. A point on the surface of the drop is given by $(R(\theta,\phi),\theta,\phi)$ in the spherical coordinate system. The origin is located below the solid surface when $\Theta_A < \frac{1}{2}\pi$, as illustrated. The solid surface is located at $z = \cos\Theta_A$. The vector $\boldsymbol{i}$ points in the direction down the inclined surface, i.e. the gravity vector $\boldsymbol{g}$ is given by

$$\boldsymbol{g} = g\sin\gamma\boldsymbol{i} - g\cos\gamma\boldsymbol{k}.$$

The boundary condition at the contact line is

$$-\boldsymbol{U}_P\cdot\boldsymbol{m} = \begin{cases} \Theta-\Theta_A & (-\phi_A < \phi < \phi_A), \\ 0 & (\phi_A < \phi < \phi_R), \\ \dfrac{\kappa_R}{\kappa_A}(\Theta-\Theta_R) & (\phi_R < \phi < 2\pi-\phi_R), \\ 0 & (2\pi-\phi_R < \phi < 2\pi-\phi_A), \end{cases} \tag{2.2}$$

contact line is a straight-line segment $\begin{cases} \phi_A < \phi < \phi_R, \\ 2\pi-\phi_R < \phi < 2\pi-\phi_A, \end{cases}$

where the values of ϕ_A, ϕ_R and $\boldsymbol{U}_P$ must be determined. A detailed explanation of this boundary condition appears in §2 of Dussan V. & Chow. The local value of the contact angle and the vector $\boldsymbol{m}$ can be calculated using the formulas

$$\cos\Theta \equiv \boldsymbol{n}\cdot\boldsymbol{k} \tag{2.3}$$

and

$$\boldsymbol{m} = \frac{\left\{R^2\sin^2\theta - R\frac{\partial R}{\partial\theta}\sin\theta\cos\theta\right\}\left\{\hat{\boldsymbol{r}}\sin\theta+\hat{\boldsymbol{\theta}}\cos\theta\right\}+\hat{\boldsymbol{\phi}}R\frac{\partial R}{\partial\phi}}{\left\{\left(R^2\sin^2\theta - R\frac{\partial R}{\partial\theta}\sin\theta\cos\theta\right)^2+R^2\left(\frac{\partial R}{\partial\phi}\right)^2\right\}^{\frac{1}{2}}}, \tag{2.4}$$

where

$$\boldsymbol{n} = \frac{\hat{\boldsymbol{r}}R^2\sin\theta - \hat{\boldsymbol{\theta}}R\frac{\partial R}{\partial\theta}\sin\theta - \hat{\boldsymbol{\phi}}R\frac{\partial R}{\partial\phi}}{\left\{R^4\sin^2\theta+R^2\left(\frac{\partial R}{\partial\theta}\right)^2\sin^2\theta+R^2\left(\frac{\partial R}{\partial\phi}\right)^2\right\}^{\frac{1}{2}}}. \tag{2.5}$$

The vector $\boldsymbol{n}$ denotes the outward unit normal to the free surface. The location of the contact line will be given by $(R(\theta_{cL},\phi), \theta_{cL}, \phi)$, where the function $\theta_{cL}(\phi)$ is defined as the solution to the equation

$$\cos\Theta_A = R(\theta_{cL},\phi)\cos\theta_{cL} \tag{2.6}$$

for all values of ϕ.

The only other constraint imposed is the specification of the volume of the drop V. This is given by

$$\frac{V}{a_s^3} = \int_0^{2\pi} \left\{ \int_0^{\theta_{cL}} \int_0^R r^2 \sin\theta \, dr \, d\theta - \tfrac{1}{6} \cos^3 \Theta_A \tan^2 \theta_{cL} \right\} d\phi. \tag{2.7}$$

2.2. *Expansion of parameters*

We will only seek solutions valid in the limit as both R_e and C_a approach zero. This simplifies the mathematics quite a bit. The Navier–Stokes equation reduces to its static form

$$0 = -\nabla P + B_d(-\boldsymbol{k} \cos\gamma + \boldsymbol{i} \sin\gamma), \tag{2.8}$$

and the dynamic boundary condition at the free surface becomes

$$-P = \frac{1}{R_M}. \tag{2.9}$$

The boundary condition (2.2) at the contact line and the volume constraint (2.7) enter at this order without any obvious simplifications. No subscripts have been introduced at this point, since we will not be concerned with higher-order modes.

It is important to realize that at least four scales for the velocity have been introduced thus far: $\mu/\rho a_s$, σ/μ, κ_R and κ_A. The ratio between the first and last scales forms the Reynolds number, while the ratio between the second and last scales forms the capillary number. Although (2.8) and (2.9) are commonly identified with static fluids, this need not always be the case. For example, in the present study, motion will originate from the boundary condition (2.2) at the contact line.

The solution to (2.8) and (2.9) has the following simple form:

$$\frac{1}{R_M} = B_d\{(R\cos\theta - \cos\Theta_A)\cos\gamma - R\sin\theta\sin\gamma\} + A_s, \tag{2.10}$$

where A_s denotes an absolute constant to be determined. Two limiting solutions will be investigated. In §3 an expansion will be performed valid for small values of B_d evaluated at $\cos\Theta_R - \cos\Theta_A \equiv 0$, and for $0 < \gamma \leqslant \frac{1}{2}\pi$. The principal objective is to determine the dependence of the slope and speed at which the drop rolls down the inclined plane on the values of κ_A, κ_R and Θ_A. In §4 a solution will be obtained, valid for small values of $\cos\Theta_R - \cos\Theta_A$, for the size and shape of a drop when it is in its critical configuration. Again, the only restriction placed on γ is that $0 < \gamma \leqslant \frac{1}{2}\pi$. Both problems represent perturbations about a common base state, identified as the (00)-mode corresponding to $B_d \equiv 0$ and $\cos\Theta_R - \cos\Theta_A \equiv 0$. Its solution is presented in §2.3.

2.3. *Solution to* (00)*-mode*

At the limit of $B_d \equiv 0$ and $\cos\Theta_R - \cos\Theta_A \equiv 0$ the pressure P_{00} must be an absolute constant. Its value will be denoted by $-A_{s00}$. This implies that the drop has a constant mean radius of curvature. Since the static contact angle has a unique value Θ_A, the drop must have the shape of a spherical cap. Its radius R_{00} is then determined by the volume constraint (2.7). In summary, we have

$$P_{00} = -A_{s00} = 2, \tag{2.11}$$

$$R_{00} = 1 \tag{2.12}$$

and

$$\frac{V}{a_s^3} = \tfrac{2}{3}\pi(1 - \cos\Theta_A - \tfrac{1}{2}\cos\Theta_A \sin^2\Theta_A). \tag{2.13}$$

Here, (2.12) can be thought of as giving the explicit definition of the lengthscale a_s, and (2.13) gives a means for calculating its value upon knowing the volume of the drop.

3. The steady motion of a drop moving down an inclined plane with no contact-angle hysteresis

3.1. *Formulation of boundary-value problem*

Any inclination of the solid surface from the horizontal will cause the drop to be in motion. The magnitude of the force responsible for this behaviour is given by $B_d \sin\gamma$. It will be assumed that the unknown quantities can be expanded in an asymptotic series valid in the limit as $B_d \to 0$ of the form

$$R \sim 1 + B_d R_{10}(\theta, \phi; \gamma, \Theta_A, \kappa_A/\kappa_R) + \dots, \tag{3.1a}$$

$$A_s \sim -2 + B_d A_{s10}(\gamma, \Theta_A, \kappa_A/\kappa_R) + \dots, \tag{3.1b}$$

$$U_P \sim B_d U_{P10}(\gamma, \Theta_A, \kappa_A/\kappa_R) + \dots, \tag{3.1c}$$

where we have used the results of §2.3. Substituting the above into (2.10) and making use of (2.1) gives, to $O(B_d)$ as $B_d \to 0$,

$$\frac{\partial^2 R_{10}}{\partial\theta^2} + 2R_{10} + \frac{1}{\sin^2\theta}\frac{\partial^2 R_{10}}{\partial\phi^2} + \frac{\cos\theta}{\sin\theta}\frac{\partial R_{10}}{\partial\theta} = (\cos\theta - \cos\Theta_A)\cos\gamma - \sin\theta\cos\phi\sin\gamma + A_{s10}. \tag{3.2}$$

The expansion of the boundary condition at the contact line is a bit more elaborate. We begin by assuming an asymptotic expansion for θ_{cL} of the form

$$\theta_{cL} \sim \Theta_A + B_d \theta_{cL10}(\phi; \gamma, \Theta_A, \kappa_A/\kappa_R) + \dots \tag{3.3}$$

valid in the limit as $B_d \to 0$. Substituting (3.1*a*) and (3.3) into (2.6) gives, to $O(B_d)$ as $B_d \to 0$,

$$\theta_{cL10} = \frac{R_{10}(\Theta_A, \phi)\cos\Theta_A}{\sin\Theta_A}. \tag{3.4}$$

The expansion of the boundary condition (2.2) at the contact line follows directly upon substituting (3.1*a*, *c*) and (3.3) into (2.3), (2.4), and (2.5), and making use of (3.4). One obtains, to $O(B_d)$ as $B_d \to 0$,

$$-\frac{R_{10}(\Theta_A, \phi)\cos\Theta_A}{\sin\Theta_A} + \left.\frac{\partial R_{10}}{\partial\theta}\right|_{(\Theta_A, \phi)} = U_{P10}\,\kappa(\phi)\cos\phi, \tag{3.5}$$

where

$$\kappa(\phi) \equiv \begin{cases} 1 & (-\tfrac{1}{2}\pi < \phi < \tfrac{1}{2}\pi), \\ \dfrac{\kappa_A}{\kappa_R} & (\tfrac{1}{2}\pi < \phi < \tfrac{3}{2}\pi) \end{cases}$$

and $\boldsymbol{U}_{P10} = U_{P10}\boldsymbol{i}$.

We have assumed that $\phi_A = \phi_R = \frac{1}{2}\pi$ because $\Theta_A \equiv \Theta_R$, and that the origin of the coordinate system is placed so that the advancing and receding portions of the contact line corresponds to $-\frac{1}{2}\pi < \phi < \frac{1}{2}\pi$ and $\frac{1}{2}\pi < \phi < \frac{3}{2}\pi$ respectively.

The expansion of the volume constraint (2.7) gives

$$0 = \int_0^{2\pi}\int_0^{\Theta_A} R_{10}\sin\theta\,\mathrm{d}\theta\,\mathrm{d}\phi, \tag{3.6}$$

to $O(B_d)$ as $B_d \to 0$.

3.2. *Solution*

It is more convenient to express the above-specified boundary-value problem in terms of a new independent variable s, given by $\cos\theta$, and to introduce a new dependent variable $\bar{R}$, defined by

$$\bar{R} \equiv R_{10} - \frac{1}{3}\left\{[1 - s\ln(1+s)]\cos\gamma + \left[(1-s^2)^{\frac{1}{2}}\ln(1+s) + s\left[\frac{1-s}{1+s}\right]^{\frac{1}{2}}\right]\sin\gamma\cos\phi\right\}$$
$$-\tfrac{1}{2}A_{s10} + \tfrac{1}{2}s_A\cos\gamma, \quad (3.7)$$

where $s_A \equiv \cos\Theta_A$. The boundary-value problem defined by (3.2) and (3.5) takes on the form

$$\frac{\partial}{\partial s}\left[(1-s^2)\frac{\partial\bar{R}}{\partial s}\right] + 2\bar{R} + \frac{1}{1-s^2}\frac{\partial^2\bar{R}}{\partial\phi^2} = 0, \quad (3.8)$$

$$\left(\bar{R}s + (1-s^2)\frac{\partial\bar{R}}{\partial s}\right)\Big|_{(s_A,\phi)}$$
$$= \frac{1}{3}\left\{[1 - s_A\ln(1+s_A)]\cos\gamma + [-2 + s_A + s_A^2]\left[\frac{1-s_A}{1+s_A}\right]^{\frac{1}{2}}\sin\gamma\cos\phi\right\}$$
$$-\tfrac{1}{2}A_{s10}s_A + \tfrac{1}{2}s_A^2\cos\gamma - U_{P10}[1-s_A^2]^{\frac{1}{2}}\kappa(\phi)\cos\phi. \quad (3.9)$$

It is easily established that the general solution to (3.8) is given by

$$\bar{R} = E_0 P_1(s) + E_1 P_1^1(s)\cos\phi + \sum_{n=2}^{\infty} E_n\left[\frac{1-s}{1+s}\right]^{\frac{1}{2}n} P_1^{(n,-n)}(s)\cos n\phi, \quad (3.10)$$

where P_1, P_1^1 and $P_1^{(n,-n)}$ (Legendre, associated Legendre and Jacobi polynomials) are s, $-(1-s^2)^{\frac{1}{2}}$ and $s+n$ respectively (Abramowitz & Stegun 1964). We have used the fact that $\bar{R}$ is an even function of ϕ. Substituting (3.10) into the boundary condition (3.9), along with the Fourier expansion of $\kappa(\phi)\cos\phi$,

$$\kappa(\phi)\cos\phi = \frac{1}{\pi}\left(1 - \frac{\kappa_A}{\kappa_R}\right) + \frac{1}{2}\left(1 + \frac{\kappa_A}{\kappa_R}\right)\cos\phi + \sum_{n=1}^{\infty}\frac{2(-1)^{n+1}(1-\kappa_A/\kappa_R)}{\pi(2n-1)(2n+1)}\cos 2n\phi,$$

gives the following results:

$$U_{P10} = \frac{\frac{2}{3}[-2 + s_A + s_A^2]\sin\gamma}{[1+\kappa_A/\kappa_R][1+s_A]},$$

$$E_0 = \tfrac{1}{3}\cos\gamma\ln[1+s_A] - \tfrac{1}{2}A_{s10}s_A + \tfrac{1}{6}s_A^2\cos\gamma - \frac{1}{\pi}\left[1 - \frac{\kappa_A}{\kappa_R}\right]U_{P10}[1-s_A^2]^{\frac{1}{2}},$$

and

$$E_n = \begin{cases} \dfrac{2U_{P10}(-1)^{\frac{1}{2}n}(1-\kappa_A/\kappa_R)}{\pi(n-1)(n+1)(1-n^2)}\left(\dfrac{1+s_A}{1-s_A}\right)^{\frac{1}{2}n}[1-s_A^2]^{\frac{1}{2}} & (n = 2, 4, \ldots), \\ 0 \quad (n = 3, 5, \ldots). \end{cases}$$

Note that the above expression for $U_{\mathrm{P}10}$ can be simplified by making use of (2.13) to give

$$U_{\mathrm{P}10} = \frac{-2V\sin\gamma}{a_{\mathrm{s}}^3\pi\left[1+\frac{\kappa_{\mathrm{A}}}{\kappa_{\mathrm{R}}}\right]\sin^2\Theta_{\mathrm{A}}}. \tag{3.11}$$

The constants E_1 and $A_{\mathrm{s}10}$ are yet to be determined.

The location of the origin of the coordinate system has not been entirely specified in the solution. Its position along the x-axis must be fixed. In order to do this it is convenient to express the location of the contact line using cylindrical coordinates $(r^{\mathrm{P}}, \phi, \cos\Theta_{\mathrm{A}})$, where $r^{\mathrm{P}} \equiv R(\theta_{\mathrm{cL}}, \phi)\sin\theta_{\mathrm{cL}}$. Substituting (3.1$a$), (3.3) and (3.4) into the expression for r^{P} gives

$$r^{\mathrm{P}} = \sin\Theta_{\mathrm{A}} + B_{\mathrm{d}}\frac{R_{10}(\Theta_{\mathrm{R}}, \phi)}{\sin\Theta_{\mathrm{A}}} + \dots,$$

valid in the limit as $B_{\mathrm{d}} \to 0$. Requiring the advancing and receding portions of the contact line to be located at $-\frac{1}{2}\pi < \phi < \frac{1}{2}\pi$ and $\frac{1}{2}\pi < \phi < \frac{3}{2}\pi$ respectively necessitates that $\mathrm{d}(r^{\mathrm{P}}\sin\phi)/\mathrm{d}\phi = 0$ at $\phi = \pm\frac{1}{2}\pi$. This directly implies that $\mathrm{d}R_{10}/\mathrm{d}\phi = 0$ at $\theta = \Theta_{\mathrm{A}}$ and $\phi = \pm\frac{1}{2}\pi$, resulting in

$$E_1 = \frac{\sin\gamma}{3}\left[\ln(1+s_{\mathrm{A}}) + \frac{s_{\mathrm{A}}}{1+s_{\mathrm{A}}}\right].$$

The remaining constant $A_{\mathrm{s}10}$ is determined by substituting (3.7) and (3.10) into the volume constraint (3.6). This gives

$$A_{\mathrm{s}10} = \frac{-\frac{2}{\pi}U_{\mathrm{P}10}\left(1-\frac{\kappa_{\mathrm{A}}}{\kappa_{\mathrm{R}}}\right)(1-s_{\mathrm{A}}^2)^{\frac{3}{2}} - \frac{1}{3}\cos\gamma\,[-3+8s_{\mathrm{A}}-6s_{\mathrm{A}}^2+s_{\mathrm{A}}^4]}{-2+3s_{\mathrm{A}}-s_{\mathrm{A}}^3}.$$

4. The critical static configuration of a drop on an inclined plane with contact-angle hysteresis

4.1. *Formulation of boundary-value problem*

The following physical problems are mathematically equivalent: determining the largest angle of inclination of the solid for which the drop will not roll down its surface; and determining the volume of the largest drop that will stick to a surface inclined at a specified angle. This gives rise to the following boundary-value problem:

$$\frac{1}{R_{\mathrm{M}}} = B_{\mathrm{dc}}\{(R_{\mathrm{c}}\cos\theta - \cos\Theta_{\mathrm{A}})\cos\gamma - R_{\mathrm{c}}\sin\theta\sin\gamma\} + A_{\mathrm{sc}}, \tag{4.1}$$

$$\left.\begin{aligned} &\cos\Theta = \begin{cases} \cos\Theta_{\mathrm{A}} & (-\phi_{\mathrm{Ac}} < \phi < \phi_{\mathrm{Ac}}), \\ \cos\Theta_{\mathrm{R}} & (\phi_{\mathrm{Rc}} < \phi < 2\pi - \phi_{\mathrm{Rc}}), \end{cases} \\ &\text{contact line is a straight-line segment} \quad \begin{cases} \phi_{\mathrm{Ac}} < \phi < \phi_{\mathrm{Rc}}, \\ 2\pi - \phi_{\mathrm{Rc}} < \phi < 2\pi - \phi_{\mathrm{Ac}}, \end{cases} \end{aligned}\right\} \tag{4.2}$$

subject to the volume constraint (2.7). Equation (4.1) is just (2.10) with the subscript c appearing on the unknown parameters and dependent variable. Equation (4.2) is

equivalent to (2.2) upon setting $U_{\mathrm{P}} \equiv \mathbf{0}$. The object is to determine the functional relationships

$$\left.\begin{aligned} R_{\mathrm{c}} &= R_{\mathrm{c}}(\theta, \phi; \Theta_{\mathrm{A}}, \epsilon, \gamma), \\ A_{\mathrm{sc}} &= A_{\mathrm{sc}}(\Theta_{\mathrm{A}}, \epsilon, \gamma), \\ \phi_{\mathrm{Ac}} &= \phi_{\mathrm{Ac}}(\Theta_{\mathrm{A}}, \epsilon, \gamma), \\ \phi_{\mathrm{Rc}} &= \phi_{\mathrm{Rc}}(\Theta_{\mathrm{A}}, \epsilon, \gamma), \\ B_{\mathrm{dc}} &= B_{\mathrm{dc}}(\Theta_{\mathrm{A}}, \epsilon, \gamma), \end{aligned}\right\} \tag{4.3}$$

where $\epsilon \equiv \cos\Theta_{\mathrm{R}} - \cos\Theta_{\mathrm{A}}$.

A solution will be obtained valid in the limit $\epsilon \to 0$. Since this represents a singular limit (Dussan V. & Chow), the drop will be divided into inner and outer regions corresponding to the portions surrounding the two straight-line segments of the contact line and the rest of the drop respectively. The solution in the outer region is presented in §4.2, and that in the inner region is presented in §4.3. They are matched in §4.4.

4.2. *Outer region*

It is assumed that the leading terms of an asymptotic expansion of the functions appearing in (4.3) in the outer region have the form

$$\left.\begin{aligned} R_{\mathrm{c}} &\sim 1 + \epsilon \ln\epsilon\, R_{\mathrm{cL}}(\theta, \phi; \Theta_{\mathrm{A}}, \gamma) + \epsilon R_{\mathrm{cL}}(\theta, \phi; \Theta_{\mathrm{A}}, \gamma) + \dots, \\ A_{\mathrm{sc}} &\sim -2 + \epsilon \ln\epsilon\, A_{\mathrm{scL}}(\Theta_{\mathrm{A}}, \gamma) + \epsilon A_{\mathrm{sc1}}(\Theta_{\mathrm{A}}, \gamma) + \dots, \\ \phi_{\mathrm{Ac}} &\sim \tfrac{1}{2}\pi + \epsilon\phi_{\mathrm{Ac1}}(\Theta_{\mathrm{A}}, \gamma) + \dots, \\ \phi_{\mathrm{Rc}} &\sim \tfrac{1}{2}\pi + \epsilon\phi_{\mathrm{Rc1}}(\Theta_{\mathrm{A}}, \gamma) + \dots, \\ B_{\mathrm{dc}} &\sim \epsilon \ln\epsilon\, B_{\mathrm{dcL}}(\Theta_{\mathrm{A}}, \gamma) + \epsilon B_{\mathrm{dc1}}(\Theta_{\mathrm{A}}, \gamma) + \dots, \end{aligned}\right\} \tag{4.4}$$

valid in the limit $\epsilon \to 0$. Note that the scales appropriate for this region are those introduced in §2.1. Substituting the above expansions into (4.1), (4.2), and (2.7), and using the relationships (2.1), (2.3), (2.4), (2.5), and (2.6) gives to $O(\epsilon)$ as $\epsilon \to 0$ the following boundary-value problem:

$$\frac{\partial^2 R_{\mathrm{c1}}}{\partial\theta^2} + 2R_{\mathrm{c1}} + \frac{1}{\sin^2\theta}\frac{\partial^2 R_{\mathrm{c1}}}{\partial\phi^2} + \frac{\cos\theta}{\sin\theta}\frac{\partial R_{\mathrm{c1}}}{\partial\theta} = B_{\mathrm{dc1}}[(\cos\theta - \cos\Theta_{\mathrm{A}})\cos\gamma - \sin\theta\sin\gamma\cos\phi] + A_{\mathrm{sc1}}, \tag{4.5}$$

$$-R_{\mathrm{c1}}(\Theta_{\mathrm{A}}, \phi)\cos\Theta_{\mathrm{A}} + \left.\frac{\partial R_{\mathrm{c1}}}{\partial\theta}\right|_{(\Theta_{\mathrm{A}}, \phi)} \sin\Theta_{\mathrm{A}} = \begin{cases} 0 & (-\frac{1}{2}\pi < \phi < \frac{1}{2}\pi), \\ 1 & (\frac{1}{2}\pi < \phi < \frac{3}{2}\pi) \end{cases} \tag{4.6}$$

and

$$\int_0^{2\pi}\int_0^{\Theta_{\mathrm{A}}} R_{\mathrm{c1}} \sin\theta \,\mathrm{d}\theta\,\mathrm{d}\phi = 0, \tag{4.7}$$

where the details of the expansions of the boundary condition at the contact line and the volume constraint are similar to that given in §3.1.

As in §3.2, it is convenient to seek a solution in terms of the independent variable s, given by $\cos\theta$, and a new dependent variable $\hat{R}$, defined by

$$\hat{R} \equiv R_{\mathrm{c1}} - \tfrac{1}{3}B_{\mathrm{dc1}}\left\{[1 - s\ln(1+s)]\cos\gamma + \left[(1-s^2)^{\frac{1}{2}}\ln(1+s) + s\left(\frac{1-s}{1+s}\right)^{\frac{1}{2}}\right]\sin\gamma\cos\phi\right\} - \tfrac{1}{2}A_{\mathrm{sc1}} + \tfrac{1}{2}B_{\mathrm{dc1}}\, s_{\mathrm{A}}\cos\gamma.$$

The boundary-value problem becomes

$$\left.\begin{aligned}
&\frac{\partial}{\partial s}\left[(1-s^2)\frac{\partial \hat{R}}{\partial s}\right]+2\hat{R}+\frac{1}{1-s^2}\frac{\partial \hat{R}}{\partial \phi^2}=0,\\
&\left[\hat{R}s+(1-s^2)\frac{\partial \hat{R}}{\partial s}\right]\Big|_{(s_A,\phi)}\\
&\quad=\tfrac{1}{3}B\left\{[\ln(1+s_A)-s_A^2]\cos\gamma+[-2+s_A+s_A^2]\left[\frac{1-s_A}{1+s_A}\right]^{\frac{1}{2}}\sin\gamma\cos\phi\right\}\\
&\qquad-\tfrac{1}{2}A_{sc1}s_A+\tfrac{1}{2}B_{dc1}s_A^2\cos\gamma+\begin{cases}0 & (-\frac{1}{2}\pi<\phi<\pi),\\ -1 & (\frac{1}{2}\pi<\phi<\frac{3}{2}\pi).\end{cases}
\end{aligned}\right\} \tag{4.8}$$

The general solution to the above is

$$\hat{R}=D_0P_1(s)+D_1P_1^1(s)\cos\phi+\sum_{n=2}^{\infty}D_n\left[\frac{1-s}{1+s}\right]^{\frac{1}{2}n}P_1^{(n,-n)}(s)\cos n\phi. \tag{4.9}$$

Substituting (4.9) into (4.8) and (4.7), along with the Fourier-series representation

$$-\frac{1}{2}+\sum_{n=0}^{\infty}\frac{2(-1)^n}{\pi(2n+1)}\cos(2n+1)\phi=\begin{cases}0 & (-\frac{1}{2}\pi<\phi<\frac{1}{2}\pi),\\ -1 & (\frac{1}{2}\pi<\phi<\frac{3}{2}\pi),\end{cases}$$

gives

$$B_{dc1}=\frac{6}{\pi(s_A+2)(1-s_A)\sin\gamma}\left[\frac{1+s_A}{1-s_A}\right]^{\frac{1}{2}}, \tag{4.10}$$

$$D_0=\frac{\cot\gamma}{\pi(1-s_A)(2+s_A)}\left[\frac{1+s_A}{1-s_A}\right]^{\frac{1}{2}}\left[\frac{3s_A}{s_A+2}+2\ln(1+s_A)\right]-\frac{1}{(1-s_A)(2+s_A)},$$

$$D_n=\begin{cases}0 & (n=4,6,\ldots),\\ \dfrac{2}{\pi}\dfrac{(-1)^{\frac{1}{2}(n-1)}}{n(1-n^2)}\left[\dfrac{1+s_A}{1-s_A}\right]^{\frac{1}{2}n} & (n=3,5,\ldots)\end{cases}$$

and

$$A_{sc1}=-\frac{2}{\pi}\frac{(s_A+3)\cot\gamma}{(s_A+2)^2}\left[\frac{1+s_A}{1-s_A}\right]^{\frac{1}{2}}+\frac{1+s_A}{(1-s_A)(2+s_A)}.$$

The remaining unknown constant D_1 will be determined upon matching the inner and outer solutions.

It is of interest to note that the series appearing in (4.9) can be summed, resulting in the following analytic form:

$$\begin{aligned}
\hat{R}=D_0s-D_1(1-s^2)^{\frac{1}{2}}\cos\phi-\frac{\Omega^{\frac{1}{2}}}{2\pi}\Bigg\{&\frac{-2s}{\Omega^{\frac{1}{2}}}\tan^{-1}\left(\frac{2\Omega^{\frac{1}{2}}\cos\phi}{1-\Omega}\right)\\
&+(3s+1)\cos\phi+\left[\frac{1}{\Omega}(s-1)-s-1\right]\cos\phi\ln(1+2\Omega\cos2\phi+\Omega^2)^{\frac{1}{2}}\\
&+\left[\frac{1}{\Omega}(s-1)+s+1\right]\sin\phi\tan^{-1}\left(\frac{\Omega\sin2\phi}{1+\Omega\cos2\phi}\right)\Bigg\},
\end{aligned} \tag{4.11}$$

where

$$\Omega\equiv\frac{(1+s_A)(1-s)}{(1-s_A)(1+s)}.$$

The boundary-value problem to lowest order containing the terms with subscript cL is very similar to the one solved above. It can easily be shown that

$$\frac{\partial}{\partial s}\left[(1-s^2)\frac{\partial R_{\mathrm{cL}}}{\partial s}\right]+2R_{\mathrm{cL}}+\frac{1}{1-s^2}\frac{\partial^2 R_{\mathrm{cL}}}{\partial \phi^2}$$

$$= B_{\mathrm{dcL}}\{(s-s_{\mathrm{A}})\cos\gamma-(1-s^2)^{\frac{1}{2}}\sin\gamma\cos\phi\}+A_{\mathrm{scL}},$$

$$\left\{-R_{\mathrm{cLs}}+\frac{\partial R_{\mathrm{cL}}}{\partial\theta}[1-s_{\mathrm{A}}^2]^{\frac{1}{2}}\right\}\Bigg|_{(s_{\mathrm{A}},\,\phi)}=0 \quad (0\leqslant\phi\leqslant 2\pi),$$

and

$$\int_0^{2\pi}\int_1^{s_{\mathrm{A}}} R_{\mathrm{cL}}\,\mathrm{d}s\,\mathrm{d}\phi=0.$$

The solution is given by $B_{\mathrm{dcL}}=0$, $A_{\mathrm{scL}}=0$ and

$$R_{\mathrm{cL}}=-F\sin\theta\cos\phi,$$

where the constant F is determined upon matching the inner and outer solutions.

4.3. *Inner region*

In the outer region the primary difference between the boundary-value problem of the present study and that of Dussan V. & Chow lies in the coordinate systems. The former uses spherical coordinates while the latter uses polar coordinates. This difference disappears in the inner region where it is appropriate in both studies to use a local rectangular-Cartesian coordinate system. For this reason extensive use can be made of the results presented in Dussan V. & Chow.

The inner regions are located in the vicinity of $(1, \Theta_{\mathrm{A}}, \pm\frac{1}{2}\pi)$, using spherical coordinates. They contain the straight-line segments of the contact line. Attention will be restricted to an analysis of the inner region near the point $(1, \Theta_{\mathrm{A}}, \frac{1}{2}\pi)$. As in Dussan V. & Chow, a local rectangular Cartesian coordinate system is introduced with the origin at $(1, \Theta_{\mathrm{A}}, \frac{1}{2}\pi)$ (see figure 5). Here the coordinates $(\bar{x}_\epsilon, \bar{y}_\epsilon, \bar{z}_\epsilon)$ are given by

$$(\bar{x}_\epsilon, \bar{y}_\epsilon, \bar{z}_\epsilon)\equiv\frac{1}{\epsilon}(\bar{x},\,\bar{y},\,z-\cos\Theta_{\mathrm{A}})$$

where $(\bar{x}, \bar{y}, z)$ are scaled with a_{s}. The shape of the free surface and location of the contact line will be described by $\bar{z}_\epsilon = h_{\epsilon\mathrm{c}}(\bar{x}_\epsilon, \bar{y}_\epsilon; \Theta_{\mathrm{A}}, \epsilon, \gamma)$ and $\bar{y}_\epsilon = \overline{Y}_{\epsilon\mathrm{c}}(\bar{x}_\epsilon; \Theta_{\mathrm{A}}, \epsilon, \gamma)$, respectively. The locations of the ends of the straight-line segments of the contact line are denoted by $\bar{x}_\epsilon = \pm L_\epsilon$, where the value of L_ϵ is to be determined.

Asymptotic expansions are assumed of the form

$$h_{\epsilon\mathrm{c}} \sim h_{\epsilon 00}(\bar{x}_\epsilon, \bar{y}_\epsilon; \Theta_{\mathrm{A}}, \gamma)+\epsilon h_{\epsilon c1}(\bar{x}_\epsilon, \bar{y}_\epsilon; \Theta_{\mathrm{A}}, \gamma)+\ldots \tag{4.12}$$

and

$$\overline{Y}_{\epsilon c} \sim \overline{Y}_{\epsilon 00}(\Theta_{\mathrm{A}}, \gamma)+\epsilon\,\overline{Y}_{\epsilon c1}(\bar{x}_\epsilon; \Theta_{\mathrm{A}}, \gamma)+\ldots, \tag{4.13}$$

valid in the limit $\epsilon\to 0$. The above implies that a domain perturbation will be performed about $\bar{y}_\epsilon = \overline{Y}_{\epsilon 00}$, a different location from that used in the expansions in the outer region. The leading-order terms in the asymptotic expansions for A_{sc} and B_{dc} have already been determined in §4.2.

Substituting (4.12) and (4.13) into (4.1) and (4.2) gives rise to an infinite set of boundary-value problems. It is straightforward to show that the solution to the lowest-order mode is $h_{\epsilon 00} = (\bar{y}_\epsilon - \overline{Y}_{\epsilon 00})\tan\Theta_{\mathrm{A}}$, where the constant $\overline{Y}_{\epsilon 00}$ must be

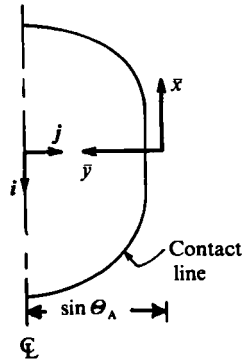

FIGURE 5. A local coordinate system scaled with a_s is constructed with origin at $(1, \Theta_A, \frac{1}{2}\pi)$ in spherical coordinates.

determined by matching the inner and outer solutions. The boundary-value problem for the next-order mode is

$$\frac{\partial^2 h_{\epsilon c1}}{\partial \bar{\bar{x}}_\epsilon^2}+\frac{\partial^2 h_{\epsilon c1}}{\partial \bar{y}_\epsilon^2}=\frac{A_{s00}}{\cos^3\Theta_A},$$

$$\left.\frac{\partial h_{\epsilon c1}}{\partial \bar{y}_\epsilon}\right|_{(\bar{\bar{x}}_\epsilon,\,\bar{Y}_{\epsilon 00})}=\begin{cases}0 & (\bar{\bar{x}}_\epsilon<-L_\epsilon|\cos\Theta_A|),\\ -\dfrac{1}{\cos^3\Theta_A\tan\Theta_A} & (\bar{\bar{x}}_\epsilon>L_\epsilon|\cos\Theta_A|)\end{cases}$$

and $$h_{\epsilon c1}(\bar{\bar{x}}_\epsilon,\,\bar{Y}_{\epsilon 00})=\tfrac{1}{2}w_{c2}\tan\Theta_A \quad (-L_\epsilon|\cos\Theta_A|\leqslant\bar{\bar{x}}_\epsilon\leqslant L_\epsilon|\cos\Theta_A|),$$

where $\bar{\bar{x}}_\epsilon\equiv\bar{x}_\epsilon|\cos\Theta_A|$, and w_{c2} appears in the asymptotic expansion for the variable denoting the width of the drop, w_c,

$$w_c\equiv 2\sin\Theta_A-2\epsilon\bar{Y}_\epsilon(0;\,\Theta_A,\epsilon,\gamma)\sim 2+\epsilon w_{c1}+\epsilon^2 w_{c2}+\ldots,$$

valid in the limit as $\epsilon\to 0$. This implies that

$$w_{c1}=-2\bar{Y}_{\epsilon 00}(\Theta_A,\gamma) \quad\text{and}\quad w_{c2}=-2\bar{Y}_{\epsilon c1}(0;\,\Theta_A,\gamma).$$

It is worth noting that the interface is located above the solid in the region $\bar{y}_\epsilon\gtrless 0$ for $\Theta_A\lesseqgtr\frac{1}{2}\pi$. This necessitates treating the two cases separately. The analysis that follows applies specifically to the case when $\Theta_A<\frac{1}{2}\pi$. The analysis appropriate when $\Theta_A>\frac{1}{2}\pi$ differs from the above only in the sign of various terms.

The above-specified boundary-value problem is mathematically equivalent to that appearing in Dussan V. & Chow upon making the following correspondence of terms

$$(h_{\epsilon 0c1},\,A_{000},\,w_{0c2})\sim(h_{\epsilon c1}\sin\Theta_A\cos^2\Theta_A,\,A_{s00}\tan\Theta_A,\,w_{c2}\sin^2\Theta_A\cos\Theta_A).$$

Hence the solution is given by

$$h_{\epsilon c1}=\frac{\bar{\bar{x}}_\epsilon^2 A_{s00}}{2\cos^3\Theta_A}+\frac{1}{\tan\Theta_A\cos^3\Theta_A}\Bigg[\Bigg[-\bar{L}_\epsilon\sinh Y\cos X\left[\frac{1}{2}+\frac{1}{\pi}\tan^{-1}\left(\frac{\cosh Y\sin X}{\sinh Y\cos X}\right)\right]$$

$$-\frac{\bar{L}_\epsilon}{2\pi}\cosh Y\sin X\,(\ln\bar{L}_\epsilon^2-2+\ln[\cosh^2 Y\sin^2 X+\sinh^2 Y\cos^2 X])$$

$$+\bar{c}_0\,Y+\tfrac{1}{2}w_{c2}\tan^2\Theta_A\cos^3\Theta_A-\tfrac{1}{4}\bar{L}_\epsilon^2 A_{s00}\tan\Theta_A$$

$$+\frac{\bar{L}_\epsilon}{\pi}[-\tfrac{1}{2}-\ln 2+\tfrac{1}{2}\ln \bar{L}_\epsilon^2]\,e^{-Y}\sin X+\bar{c}_1\sinh Y\sin X$$

$$+\tfrac{1}{4}\bar{L}_\epsilon^2 A_{s00}\,e^{-2Y}\tan\Theta_A\cos 2X+2\bar{c}_2\sinh 2Y\cos 2X$$

$$+\frac{\bar{L}_\epsilon}{2\pi}\Bigg[-e^{-Y}\sin X+2\cos X\sinh Y\tan^{-1}\left(\frac{e^{-2Y}\sin 2X}{1-e^{-2Y}\cos 2X}\right)$$

$$+2\sin X\cosh Y\ln(1-2e^{-2Y}\cos 2X+e^{-4Y})^{\frac{1}{2}}\Bigg]$$

$$+\sum_{k=1}^{\infty}2\bar{c}_{2k+1}\sinh(2k+1)Y\sin(2k+1)X\Bigg], \tag{4.14}$$

where

$$\bar{L}_\epsilon\equiv L_\epsilon\cos\Theta_A,\quad \bar{\bar{x}}_\epsilon=\bar{L}_\epsilon\cosh Y\sin X\quad\text{and}\quad \bar{y}_\epsilon=\bar{Y}_{\epsilon 00}+\bar{L}_\epsilon\sinh Y\cos X.$$

The constants $\bar{L}_\epsilon$ and $\{\bar{c}_k;\ k=0,1,\ldots\}$ are yet to be determined.

Three additional constraints must be imposed on (4.14) in order for it to be an acceptable solution: (i) the value of the contact angle along the straight-line segments of the contact line must lie within the interval $[\Theta_R,\Theta_A]$; (ii) the tangent of the contact line must be continuous at the endpoints of the straight-line segments; and (iii) the largest and smallest values of $\bar{y}$ corresponding to points along the contact line must occur along the straight-line segments.

It can easily be shown that the first constraint implies

$$-1\leqslant\bar{L}_\epsilon\tan\Theta_A\cos X-\frac{1}{\pi}(X+\tfrac{1}{2}\pi)\leqslant 0$$

for $-\frac{1}{2}\pi\leqslant X\leqslant\frac{1}{2}\pi$. This, in turn, implies that

$$\bar{L}_\epsilon\leqslant\frac{1}{\pi\tan\Theta_A}. \tag{4.15}$$

The second constraint requires that

$$\frac{d\bar{Y}}{d\bar{\bar{x}}_\epsilon}\to 0\quad\text{as }\bar{\bar{x}}_\epsilon\to\pm\bar{L}_\epsilon\quad\text{for }|\bar{\bar{x}}_\epsilon|>\bar{L}_\epsilon.$$

This can easily be evaluated using the expression

$$-\cos^3\Theta_A\tan^2\Theta_A\frac{d\bar{Y}_{\epsilon c1}}{d\bar{\bar{x}}_\epsilon}$$

$$=\frac{\pm\tan\Theta_A\cos^3\Theta_A}{(\bar{\bar{x}}_\epsilon^2-\bar{L}_\epsilon^2)^{\frac{1}{2}}}\frac{d}{dY}\left(h_{\epsilon c1}-\frac{\bar{\bar{x}}_\epsilon^2 A_{s00}}{2\cos^3\theta_A}\right)\Bigg|_{(\pm\frac{1}{2}\pi,\,Y)}+\bar{\bar{x}}_\epsilon A_{s00}\tan\Theta_A \tag{4.16}$$

along with (4.14). It can be concluded that

$$\bar{c}_0+\tfrac{1}{2}\bar{L}_\epsilon^2 A_{s00}\tan\Theta_A-4\bar{c}_2=0 \tag{4.17}$$

and

$$\bar{c}_1=\frac{\bar{L}_\epsilon}{2\pi}\ln\frac{\bar{L}_\epsilon}{2}. \tag{4.18}$$

Finally, it can readily be shown that the third constraint is equivalent to

$$\frac{d^2\bar{Y}_{\epsilon c1}}{d\bar{\bar{x}}_\epsilon^2}\geqslant 0\quad\text{as }\bar{\bar{x}}_\epsilon\to\pm\bar{L}_\epsilon\quad\text{for }|\bar{\bar{x}}_\epsilon|>\bar{L}_\epsilon.$$

Upon differentiating (4.16) with respect to $\bar{\bar{x}}_\epsilon$, it can be shown that this inequality implies

$$\pm \frac{\bar{L}_\epsilon}{\pi} \geqslant -2\bar{c}_0. \tag{4.19}$$

The remaining unknown constants $\{\bar{c}_k;\ k = 0, 1, \ldots\}$, $\bar{L}_\epsilon$, $\bar{Y}_{\epsilon 00}$, D_1 and F are determined by matching the inner and outer solutions. This is accomplished by first expressing the inner solution (4.12), in terms of the variables $(\bar{x}, \bar{y})$ and rearranging it as an asymptotic expansion in terms of the sequence $\{1, \epsilon \ln \epsilon, \epsilon, \ldots\}$. The local form of the outer solution h_c is obtained from the expression

$$h_c \equiv (1 + \epsilon \ln \epsilon\, R_{cL}(\theta, \phi) + \epsilon R_{c1}(\theta, \phi) + \ldots) \cos\theta - \cos\Theta_A,$$

where the variables (θ, ϕ), represented by

$$\theta \sim \theta_0(\bar{x}, \bar{y}) + \epsilon \ln \epsilon\, \theta_L(\bar{x}, \bar{y}) + \epsilon\theta_1(\bar{x}, \bar{y}) + \ldots,$$

$$\phi \sim \phi_0(\bar{x}, \bar{y}) + \epsilon \ln \epsilon\, \phi_L(\bar{x}, \bar{y}) + \epsilon\phi_1(\bar{x}, \bar{y}) + \ldots,$$

must satisfy the equations

$$\bar{x} = (1 + \epsilon \ln \epsilon\, R_{cL}(\theta, \phi) + \epsilon R_{c1}(\theta, \phi) + \ldots) \sin\theta \cos\phi,$$

$$\sin\Theta_A - \bar{y} = (1 + \epsilon \ln \epsilon\, R_{cL}(\theta, \phi) + \epsilon R_{c1}(\theta, \phi) + \ldots) \sin\theta \sin\phi.$$

Equating these forms of the outer and inner solutions up to and including $O(\epsilon)$ as $\epsilon \to 0$ gives the following:

$$\bar{c}_0 = \frac{1}{2\pi^2} \cot\Theta_A, \quad \bar{c}_1 = \frac{|\cos\Theta_A|}{2\pi^2 \sin\Theta_A} \ln\left[\frac{|\cos\Theta_A|}{2\pi \sin\Theta_A}\right],$$

$$\bar{c}_2 = \frac{-1}{8\pi^2} \cot\Theta_A, \quad \{\bar{c}_{2k+1} = 0;\ k = 1, 2, \ldots\},$$

$$F = \frac{1}{\pi \sin\Theta_A}, \quad L_\epsilon = \frac{1}{\pi \sin\Theta_A},$$

$$D_1 = \frac{B_{dc1} \sin\gamma}{3} \left\{\ln(1 + \cos\Theta_A) + \frac{\cos\Theta_A}{1 + \cos\Theta_A}\right\} - \frac{3\cos\Theta_A - 1}{2\pi \sin\Theta_A}$$
$$+ \frac{1}{\pi \sin\Theta_A} \ln\frac{2}{\sin\Theta_A} + \frac{1 - \ln(2\pi \sin\Theta_A)}{\pi \sin\Theta_A},$$

$$\bar{Y}_{\epsilon 00} = \frac{1}{\cos\Theta_A + 2}\left[-\frac{\cot\gamma}{\pi(\cos\Theta_A + 2)} - \frac{1}{2\sin\Theta_A}\right],$$

where the expressions for F, L_ϵ, D_1 and $\bar{Y}_{\epsilon 00}$ are valid for $0 < \Theta_A < \pi$.

5. Results

The results of §§3 and 4 can be combined, as demonstrated by Dussan V. & Chow, to describe the state of a drop, valid for the general case when $\Theta_A \neq \Theta_R$, rolling down a plane whose angle of inclination slightly exceeds its critical value. The form of the solution for either R, A_s, ϕ_A, ϕ_R or U_P can be expressed as

$$\mathscr{F}\left(\gamma, B_d, \Theta_A, \Theta_R, \frac{\kappa_A}{\kappa_R}\right) \sim \mathscr{F}_{00} + \epsilon \ln \epsilon\, \mathscr{F}_{cL}(\Theta_A) + \epsilon\mathscr{F}_{c1}(\gamma, \Theta_A)$$
$$+ [B_d - \epsilon B_{dc1}(\gamma, \Theta_A)]\, \mathscr{F}_{10}\left(\gamma, \Theta_A, \frac{\kappa_A}{\kappa_R}\right) + \ldots, \tag{5.1}$$

where $\mathscr{F}$ denotes any one of the aforementioned variables.

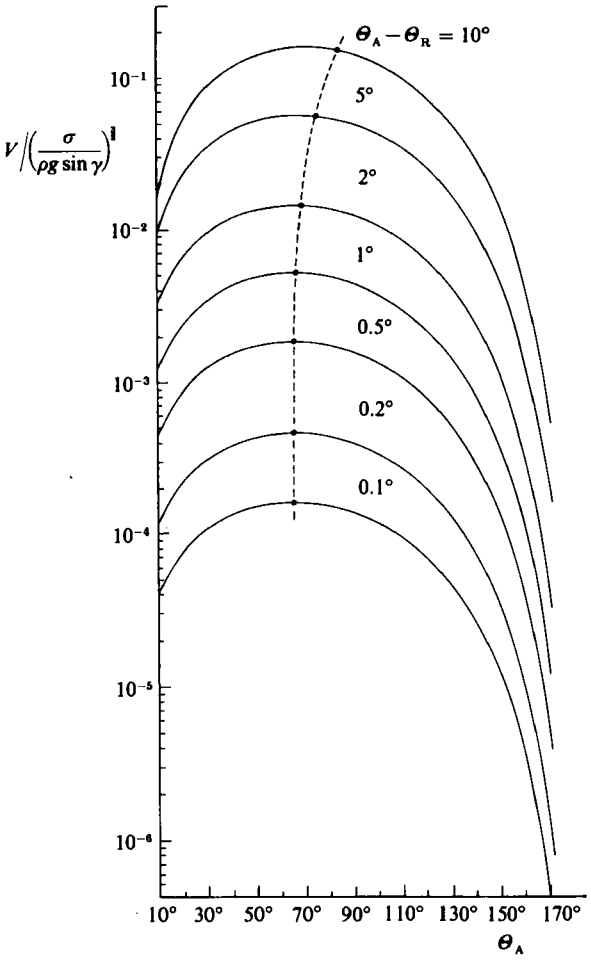

FIGURE 6. A plot of (5.3), indicating the dependence on the parameters Θ_A and Θ_R of the dimensionless volume $V(\rho g \sin\gamma/\sigma)^{\frac{3}{2}}$ of the largest drop that can stick to the solid.

The speed (in dimensional form) at which the drop rolls down the surface of the solid U_D is given by $-U_P \kappa_A$. Substituting (3.11) into (5.1) implies that

$$U_D \sim \frac{2V \sin\gamma}{a_s^3 \pi \left(\frac{1}{\kappa_A} + \frac{1}{\kappa_R}\right) \sin^2 \Theta_A} \left[\frac{\rho g a_s^2}{\sigma} - \frac{6(\cos\Theta_R - \cos\Theta_A)(1+\cos\Theta_A)^{\frac{1}{2}}}{\pi(\cos\Theta_A + 2)(1-\cos\Theta_A)^{\frac{3}{2}} \sin\gamma}\right]. \tag{5.2}$$

According to this expression, the speed of the drop should increase without bound as $\Theta_A \to 0$ and π, for fixed values of $B_d - \epsilon B_{dc1}$. However, (5.2) is only valid to $O(1)$ as the relevant capillary number $U_D \mu/\sigma$ approaches zero. These singular limits should disappear upon including the lowest-order effects due to viscosity. The volume of the largest drop that can stick to the surface of the solid inclined at a given angle γ can be calculated directly by substituting (4.4) and (4.10) into (2.13), giving

$$\left(\frac{\rho g \sin\gamma}{\sigma}\right)^{\frac{3}{2}} V \sim \left(\frac{96}{\pi}\right)^{\frac{1}{2}} \frac{(\cos\Theta_R - \cos\Theta_A)^{\frac{3}{2}}(1+\cos\Theta_A)^{\frac{3}{4}}(1-\frac{3}{2}\cos\Theta_A + \frac{1}{2}\cos^3\Theta_A)}{(\cos\Theta_A + 2)^{\frac{3}{2}}(1-\cos\Theta_A)^{\frac{9}{4}}}. \tag{5.3}$$

To illustrate some implications of this expression, the variation of $(\rho g \sin\gamma/\sigma)^{\frac{1}{3}} V$ with θ_A for several fixed values of $\theta_A - \theta_R$ ranging between 0.1° and 10° has been plotted in figure 6. This form of presentation was chosen because the appearance of hysteresis, $\theta_A \neq \theta_R$, is usually associated with either surface roughness or chemical inhomogeneity such as that which would be created by scratches or by dirt. Therefore the magnitude of the hysteresis, $\theta_A - \theta_R$, may in some sense be thought of as being an inverse measure of the amount of labour and expense necessary to manufacture the solid surface. The physical significance of the range chosen for $\theta_A - \theta_R$ in figure 6 is as follows. The smallest value, 0.1°, coincides with the limit of the accuracy of the most sensitive devices used for measuring static contact angles. However, due to variations introduced by repeated measurements with different samples of seemingly the same surface, it is found that the reproducibility of the measurements on very carefully prepared surfaces is rarely less than 1°–2°. On the other hand, 10° was chosen as the maximum value for $\theta_A - \theta_R$ since the solution is only valid for small values of $\cos\theta_R - \cos\theta_A$. Larger values of $\theta_R - \theta_A$ are quite common; in fact, it is not unusual to find a material system with a hysteresis as large as 150°.

Each curve in figure 6 identifies the drop with largest volume that can stick to the surface for various values of θ_A. The most prominent characteristic in the curves is the existence of a maximum occurring approximately at $\theta_A \approx 65.53° + 1.94(\theta_A - \theta_R)$, giving a value for $(\rho g \sin\gamma/\sigma)^{\frac{1}{3}} V$ of about $2.64(\cos\theta_R - \cos\theta_A)^{\frac{3}{2}}$; see the dashed line in the figure. (The slight discrepancies between the maxima in the curves and the values indicated by the above relationships are probably of the same order as the inaccuracy of the results due to its being only the first term in an asymptotic solution.) Hence drops with volumes greater than that value, regardless of the value of θ_A, and for a specified amount of hysteresis, cannot stick to an inclined solid surface. In general, if it is desired to minimize the value of the largest drop that can stick to a surface, then the shape of the curves in figure 6 indicates that either one must be willing to incur 'great expense' by creating a solid surface with very small hysteresis, or choose a material system so that θ_A takes on a relatively large value. Thus a solid surface with $\theta_A - \theta_R = 1.0°$ will not let a drop stick to it with scaled volume greater than 0.0052, regardless of the identity of the liquid; while a 'less expensive' surface with $\theta_A - \theta_R = 10°$ will exhibit the same characteristic only for liquids with $\theta_A \gtrsim 163°$. Finally, the results presented in figure 6 make possible a quick, sensitive and convenient experimental technique for determining the hysteresis of a solid when its value happens to be small by simply requiring the measurement of the volume of the largest drop that can stick to its surface.

Also of practical interest is the size of the area of the solid wetted by the drop. This may be important in various problems such as determining the rate of growth of condensing drops, or the extent to which a given amount of spray will wet a surface. A dimensionless form of the wetted area, $B_d \sin^2\theta_A$, to lowest order, is obtained by substituting (4.9) into (4.4) to give

$$B_d \sin^2\theta_A \sim \frac{6}{\pi \sin\gamma} \frac{(\cos\theta_R - \cos\theta_A)(1+\cos\theta_A)^{\frac{3}{2}}}{(\cos\theta_A + 2)(1-\cos\theta_A)^{\frac{1}{2}}} \tag{5.4}$$

(see figure 7). It is of interest to note that $B_d \sin^2\theta_A$ is a monotonically decreasing function of θ_A for fixed values of $\theta_A - \theta_R$, and doesn't possess a maximum as in the case for $(\rho g \sin\gamma/\sigma)^{\frac{1}{3}} V$. When $\theta_A \leqslant \frac{1}{2}\pi$, $B_d \sin^2\theta_A$ also can be used to determine the minimum number of drops required to cover a solid surface of specified size; however, this is not true when $\theta_A > \frac{1}{2}\pi$. For this latter case a better estimate can be obtained directly from B_d (see figure 8).

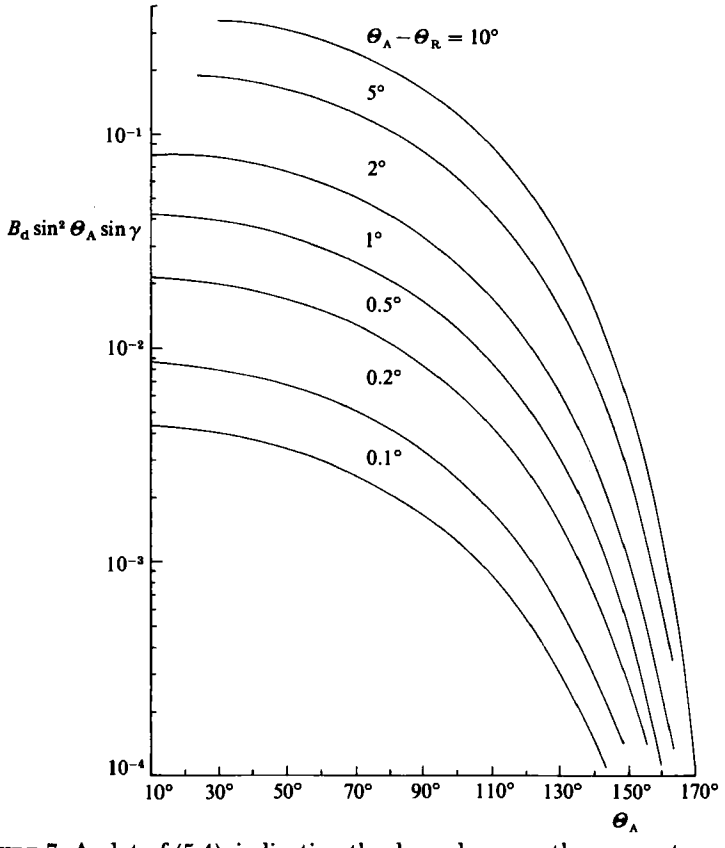

FIGURE 7. A plot of (5.4), indicating the dependence on the parameters γ, θ_A and θ_R of the dimensionless area $B_d \sin^2\theta_A$ of the solid wetted by the largest drop.

The shape of the contact line can readily be calculated using the expansion procedure outlined at the beginning of §3, along with (5.1). The radial polar coordinate, scaled by a_s for points on the contact line, r^P, is given by

$$\frac{r^P}{\sin\theta_A} \sim 1 + \frac{\epsilon \ln\epsilon}{\sin^2\theta_A} R_{cL}(\theta_A, \phi) + \frac{\epsilon}{\sin^2\theta_A} R_{c1} + (B_d - \epsilon B_{dc1}) \frac{R_{10}(\theta_A, \phi)}{\sin^2\theta_A} + \dots, \quad (5.5)$$

where

$$R_{cL} = -\frac{\cos\phi}{\pi}, \quad (5.6a)$$

$$R_{c1}(\theta_A, \phi) = -\overline{Y}_{\epsilon 00} \sin\theta_A + \frac{2\cos\phi}{\pi(\cos\theta_A + 2)(1 - \cos\theta_A)} [(1 + \cos\theta_A) \ln(1 + \cos\theta_A) + \cos\theta_A]$$
$$- \left[D_1 \sin\theta_A + \frac{3}{2\pi} \cos\theta_A + \frac{1}{2\pi} \right] \cos\phi + \frac{1}{\pi} \cos\phi \ln|2\cos\phi| + \Delta, \quad (5.6b)$$

$$R_{10}(\theta_A, \phi) = \frac{(1 - \cos\theta_A)^2 \cos\gamma}{6(\cos\theta_A + 2)} - \frac{U_{P10} \sin\theta_A}{\pi} \left[1 - \frac{\kappa_A}{\kappa_R} \right] \left[\frac{-1}{2 + \cos\theta_A} \right.$$
$$\left. + 2 \sum_{n=1}^{\infty} (-1)^n \frac{(\cos\theta_A + 2n) \cos 2n\phi}{(4n^2 - 1)^2} \right], \quad (5.6c)$$

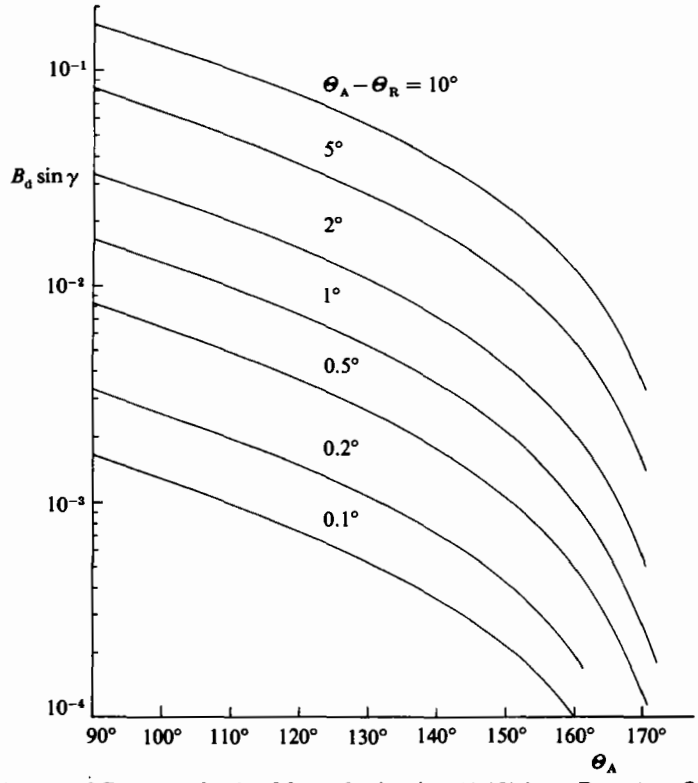

FIGURE 8. A plot of $B_d \sin\gamma$ obtained by substituting (4.10) into $B_d \sim (\cos\Theta_R - \cos\Theta_A) B_{dc1}$.

and

$$\Delta \equiv \begin{cases} \left(\frac{1}{2} - \frac{\phi}{\pi}\sin\phi\right)\cos\Theta_A & (-\tfrac{1}{2}\pi < \phi < \tfrac{1}{2}\pi), \\ -\left(\frac{1}{2} + \frac{1}{\pi}(\phi - \pi)\sin\phi\right)\cos\Theta_A & (\tfrac{1}{2}\pi < \phi < \tfrac{3}{2}\pi). \end{cases} \tag{5.6d}$$

The explicit forms for $\overline{Y}_{\epsilon 00}$ and D_1 appear at the end of § 4.3.

The effects of hysteresis and motion on the shape of the contact line can best be illustrated by examining them separately. The most obvious immediate distinguishing feature is that the perturbation to the circular shape created by the hysteresis is asymmetric with respect to the $x = 0$ plane, while the change in shape due to the motion of the drop rolling down the surface is symmetric with respect to the $x = 0$ plane. The portion of R_{10} that depends on ϕ is illustrated in figure 9. The length L_D and width w of the drop, scaled with a_s, are given by

$$\frac{L_D}{2\sin\Theta_A} \sim 1 - \epsilon\overline{Y}_{\epsilon 00} + (B_d - \epsilon B_{dc1})\left[\left[\frac{\cos\gamma}{6\sin^2\Theta_A}(2 - 3\cos\Theta_A + \cos^3\Theta_A)\right.\right.$$
$$\left.\left. + \tfrac{1}{2}A_{s10} - \frac{U_{P10}}{\pi\sin\Theta_A}\left(1 - \frac{\kappa_A}{\kappa_R}\right)(\tfrac{1}{4}\pi\cos\Theta_A - \overline{G} + \tfrac{1}{2})\right]\right],$$

$$\frac{w}{2\sin\Theta_A} \sim 1 - \epsilon\overline{Y}_{\epsilon 00} + (B_d - \epsilon B_{dc1})\left[\left[\frac{\cos\gamma}{6\sin^2\Theta_A}(2 - 3\cos\Theta_A + \cos^3\Theta_A)\right.\right.$$
$$\left.\left. + \tfrac{1}{2}A_{s10} - \frac{U_{P10}}{\pi\sin\Theta_A}\left(1 - \frac{\kappa_A}{\kappa_R}\right)(\tfrac{1}{8}\pi^2\cos\Theta_A + \tfrac{1}{2})\right]\right].$$

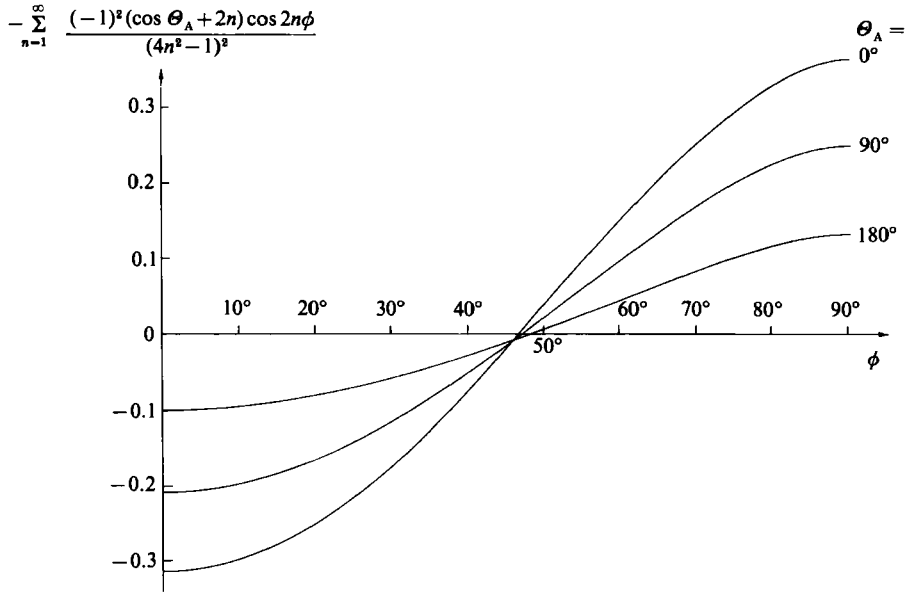

FIGURE 9. A plot of $\sum_{n=1}^{\infty} (-1)^{n+1} \frac{(\cos\Theta_A+2n)}{(4n^2-1)^2} \cos 2n\phi$

which gives that portion of the shape of the contact line resulting from the drop moving down the inclined plane that depends on ϕ; see (5.5) and (6.6).

A measure of the relative differences in the shape of the drop for $\bar{x} \geqslant 0$ as compared with $\bar{x} \leqslant 0$ is reflected in the value of δ defined by $(r^P(0)-r^P(\pi))/2\sin\Theta_A$:

$$\delta \sim -\frac{\epsilon \ln\epsilon}{\pi \sin^2\Theta_A} + \frac{\epsilon}{\sin^2\Theta_A}\left\{\frac{2}{\pi(\cos\Theta_A+2)(1-\cos\Theta_A)}\right.$$
$$\left.\times[(1+\cos\Theta_A)\ln(1+\cos\Theta_A)+\cos\Theta_A]-D_1\sin\Theta_A-\frac{3}{2\pi}\cos\Theta_A-\frac{1}{2\pi}+\frac{1}{\pi}\ln 2\right\}.$$

Hence for very small values of ϵ the front of the drop, i.e. the portion of the contact line with contact angle greater than or equal to Θ_A, is longer than its rear.

Probably the most useful direct extension of these calculations from a practical point of view would be to remove the restriction imposed by assuming that $\cos\Theta_R - \cos\Theta_A$ is a small parameter.

It is a pleasure to acknowledge the extensive efforts of B. I. Dussan V. in performing the calculations for figures 6–9.

This work was supported by the U.S. Army Research Office under grant DAAG 29-82-K-0128.

REFERENCES

ABRAMOWITZ, M. & STEGUM, I. A. 1964 *Handbook of Mathematical Functions*. National Bureau of Standards.

BIKERMAN, J. J. 1950 Sliding of drops from surfaces of different roughnesses. *J. Coll. Sci.* **5**, 349.

DUSSAN, V., E. B. & CHOW, R. T.-P. 1983 On the ability of drops or bubbles to stick to non-horizontal surfaces of solids. *J. Fluid Mech.* **137**, 1.

FURMIDGE, C. G. L. 1962 Studies at phase interfaces. I. The sliding of liquid drops on solid surfaces and a theory of spray retention. *J. Coll. Sci.* **17**, 309.